

Investigation of the mechanism of switching a short vacuum gap using an auxiliary spark discharge

© S.G. Davydov, A.N. Dolgov, A.A. Kozlov, R.Kh. Yakubov

Dukhov All-Russia Research Institute of Automatics,
127055 Moscow, Russia
e-mail: vnii4@vniia.ru

Received May 21, 2021

Revised July 16, 2021

Accepted August 2, 2021

The ionization of a rarefied gas in a short gap by a stream of short-wave radiation and fast electrons from the plasma of an auxiliary spark discharge along the dielectric surface is detected, sufficient to initiate an arc discharge in the gap. The density of the ionizing flow of particles and radiation determines the delay time of the switching gap in relation to the start of the auxiliary discharge. With an increase in the initial concentration of free electrons in the main discharge gap, the transition time to an arc discharge is reduced, due to the development of instabilities.

Keywords: plasma, arc discharge, spark discharge, ionization, instability.

DOI: 10.21883/TP.2022.15.55262.153-21

Introduction

The interest in surface dielectric spark discharge in vacuum has been stimulated by its successful application in high current and high voltage electronics for switching and opening circuits [1]. For example, a spark discharge across a dielectric surface is used as the initiator of the commutation process in vacuum dischargers, i.e. to create a conductive medium in the vacuum gap to be commuted. It is generally assumed that this medium is the plasma of the auxiliary spark discharge itself, which is formed from the erosion products of the dielectric and electrode material.

The purpose of this work — is to find out the key mechanism of short vacuum gap switching, which determines the tripping speed of a compact spark vacuum discharger.

1. Experimentation with the switchboard layout

An important parameter for vacuum spark discharger is the delay time between the start of the auxiliary spark discharge breakdown over the dielectric surface when the control voltage pulse is applied to the ignition unit and the starts of commutated current flowing through the gaps. Changing the pressure in the vacuum chamber and the distance between the ignition unit and the main discharge gap can result in a significant change in the delay time.

An open discharger layout was used for the experimental studies, which differs in that the electrode systems of the auxiliary discharge on the dielectric surface (ignition unit) and the main discharge switching the external circuit are spatially separated, but galvanically connected. The operating range of the residual gas pressure was 10^{-3} – 10^2 Pa. The used range of distances from the ignition node including ignition electrode, separating dielectric and cathode № 1, to

the main discharge gap including anode and cathode № 2, was 0.25–6.8 cm. Cathode № 2 and anode — discs with a diameter of 5 mm with a 3 mm diameter hole. The length of the discharge gap between cathode № 2 and anode is 1 mm. Dielectric thickness is 0.1 mm, material — ceramics. Electrode material — stainless steel (Fig. 1).

To initiate the switching process, a positive voltage pulse with an amplitude of 3.5 kV and a slope of $(1-2) \cdot 10^9$ V/s is applied to the ignition electrode relative to the grounded cathode. This results in a breakdown on the cylindrical dielectric surface along the shortest possible path between adjacent electrodes, and an auxiliary spark discharge is developed (Fig. 2).

The current amplitude is 4–6 A with a current pulse duration of about 20 ns. The plasma formed by the erosion products creates a conductive medium in the gap between cathode № 2 and the anode. The current switched by the discharger layout is a single half-period sinusoidal current

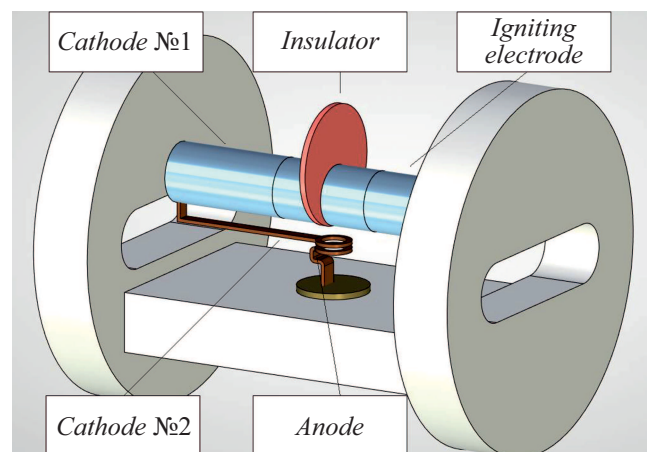


Figure 1. Research layout of a double cathode discharge device.

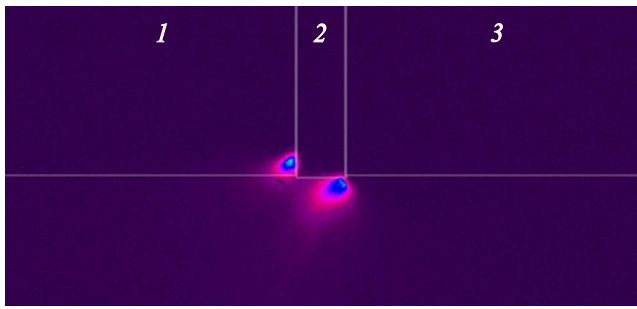


Figure 2. Images of the spark discharge in the ignition assembly of the discharger layout, taken with a high-speed camera in the visible spectrum range: 1 — cathode, 2 — dielectric insert, 3 — ignition electrode. Exposure $60\ \mu\text{s}$. On the left, you can see the bright cathode spot and the plasma of the cathode torch, on the right — the anode spot. In the space between them and below, there is an illuminated dielectric insert surface between the ignition electrode and the cathode № 1.

pulse with an amplitude of $1.5\ \text{kA}$ and a duration of $1\ \mu\text{s}$. The recorded voltages in the discharger circuit were measured with a capacitive or resistive voltage divider. The strength of the currents to be recorded was determined by measuring the voltage across low-inductance resistors rated at $0.1\text{--}100\ \Omega$.

From the data obtained in the experiments, the dependence (Fig. 3, *a*) of the delay of the arc discharge commutation to the external circuit on the residual gas pressure at different distances from the ignition point to the main discharge gap was plotted. The delay was measured as the time interval from the moment of dielectric surface breakdown in the ignition node (the moment when the ignition voltage starts to drop abruptly) to the moment when the commutated current occurs in the external circuit.

Two characteristic groups of points can be identified in the graph: for distances of $0.25\ \text{cm}$ (delay $\sim 0.1\ \mu\text{s}$) and for distances of $\geq 0.4\ \text{cm}$ (delay $\sim 1\ \mu\text{s}$). The observed delays, as is easy to see, cannot be explained by the thermal motion of the plasma from the ignition node alone (thermal velocity of plasma propagation is $\sim 10^3\ \text{m/s}$, based on its temperature not exceeding $1.5\ \text{eV}$ [2]) or the mechanism of ambipolar plasma diffusion into vacuum (corresponding velocity is $\sim 10^4\ \text{m/s}$ [3]). Firstly, the delay duration is not proportional to the distance from the ignition point. Secondly, for large distances, at least greater than $3.8\ \text{cm}$, the recorded delay time is too short. Further, if we analyze the same dependence, but already represented in semi-logarithmic scale (Fig. 3, *b*), we see that the pressure dependence is clearly expressed for distances from $0.4\ \text{cm}$ and more and tends to decrease with increasing residual gas pressure.

For long distances, the gap closes too quickly for this to be a matter of an incoming plasma closure. It can be assumed that in the initial stage of the commutation process, the ionization of the residual gas by short-wave radiation and fast electrons (with energy $\sim 100\ \text{eV}$ [4])

emitted from the auxiliary discharge plays a certain role, for which there is quite good reason [5–7]. Due to the fact that the free path of both quanta and electrons is several orders of magnitude larger than the size of the discharge gap, in the medium of weakly ionized residual gas, a weak-current volumetric discharge initially arises, for example, glowing, which undergoes spontaneous contraction, i.e. compression of the current channel as a result of the development of cathode layer instability, ionization-overheating instability or instability of another type [8–10], and then passes into arc. The experiment shows that as the residual gas pressure increases, the delay time decreases. This indicates that the higher the initial concentration of charged current-carrying particles due to the ionization of the residual gas, the faster the transition from volumetric discharge to arc discharge. And the dependence has some threshold character: exceeding the threshold of the initial concentration of charged particles, associated with a decrease in the distance between the ignition node and the main discharge gap (Fig. 3, *b*), leads to a sharp change in the delay time and character of the dependence.

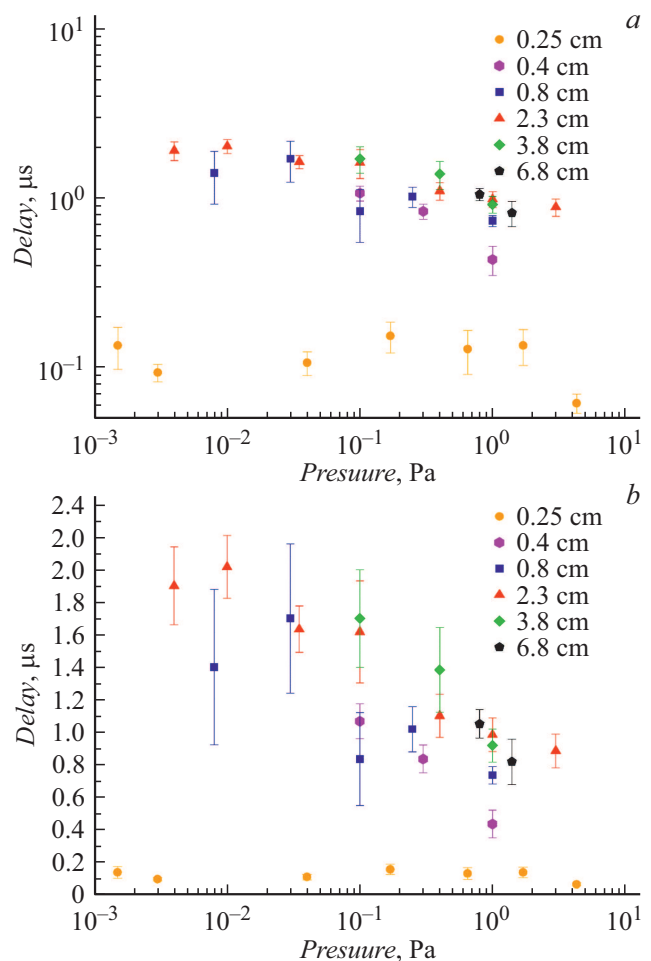


Figure 3. Dependence of arcing delay on residual gas pressure at different distances from the ignition point to the main discharge gap: *a* — in logarithmic scale; *b* — in semi-logarithmic scale.

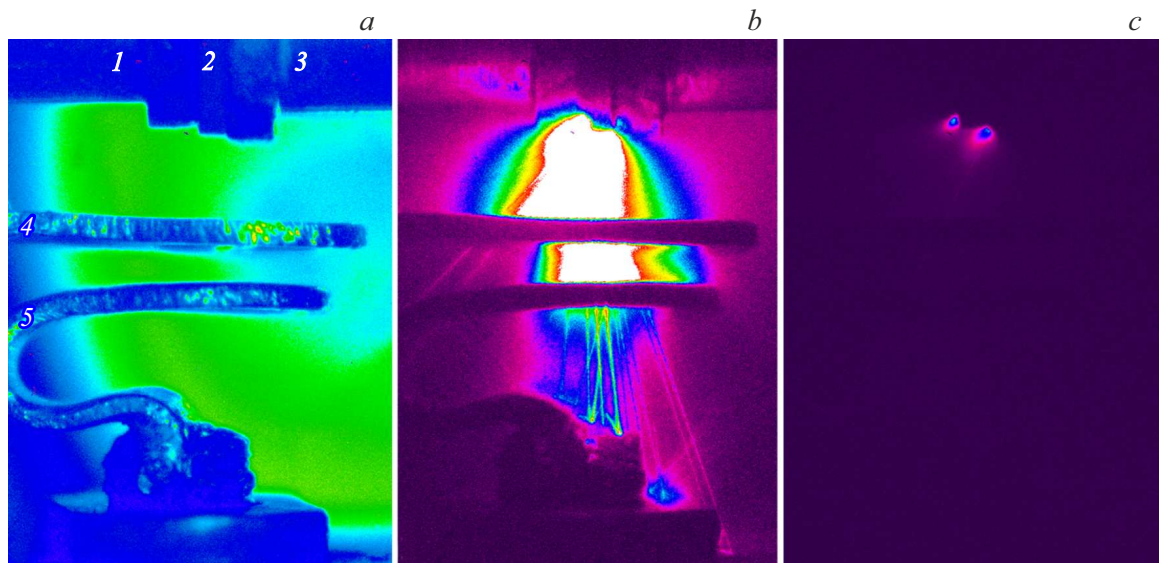


Figure 4. Photographs taken with a speed camera: *a* — layout of the discharger with no discharge and illumination from an external source: 1 — cathode № 1, 2 — dielectric insert, 3 — ignition electrode, 4 — cathode № 2, 5 — anode; *b* — discharge image in mock-up discharge at positive polarity anode potential (+100 V); *c* — discharge image in the discharger layout at negative polarity of the anode potential (−100 V).

An additional experiment was carried out, in which the anode potential was inverted, and high-speed photography of the discharge in the discharger layout was carried out (Fig. 4).

It turned out that the fact of the discharge ignition depends on the polarity of the voltage applied to the electrode gap. With negative anode polarity, the discharge in the main discharge gap ignited very rarely. Therefore, it can be concluded that the electrons emitted by the ignition unit play the main role in the development of the discharge. If the anode potential is negative, the electrons cannot enter the main discharge gap and ionize the residual gas. It should be noted that in some cases the discharge does ignite, apparently due to the ionizing effect of the shortwave radiation of the initiating discharge.

Let's make some assessments. At the minimum residual gas pressure in our experiments 10^{-3} Pa, the concentration of neutral particles in it will be about $n_0 \approx 10^{17} \text{ m}^{-3}$. The neutral particle ionization cross section of the residual gas can be taken to be $\sigma_e \approx 10^{-20} \text{ m}^2$ for electron impact ionization and $\sigma_{ph} \approx 10^{-21} \text{ m}^2$ for photoionization [4]. It can be seen that, other things being equal, photoionization is less likely. The free path for fast electrons in this case is $\lambda \approx 1/n_0\sigma_e \approx 10^3 \text{ m}$. Given the length of the commuting gap $d \approx 10^{-3} \text{ m}$ we get for the ionizing collision probability $d/\lambda \approx 10^{-6}$. The number of electrons emitted by a single explosive electron emission center and accelerated in the anode field is estimated by the value $N \approx 10^{15}$ [3]. Let's assume that the volume of the region where the effective ionization of neutral particles of the residual gas occurs in our case is $V \approx d^3 = 10^{-9} \text{ m}^3$. The concentration of charged particles produced in the residual gas by fast elec-

trons will be $n \approx (N/V) \cdot (d/\lambda) \approx 10^{15} \text{ m}^{-3}$. The Debye radius, assuming $kT \approx 1.5 \text{ eV}$, will be $r_D = (\epsilon_0 kT / e^2 n)^{1/2} \approx 10^{-4} - 10^{-3} \text{ m} < d$, where ϵ_0 — dielectric constant, k — Boltzmann constant, T — temperature of chaotic motion of free electrons, e — electron charge. Thus, at residual gas pressures of $\geq 10^{-3}$ Pa, it is quite possible for a conductive medium — plasma to form in the way described above. However, if one calculates the speed of electron current drift on the basis of the required current $\sim 10 \text{ A}$ [3] to produce a single center of electron explosive emission, it will be too high, i.e. much higher than the ionic sound speed. Consequently, Langmuir oscillations will be excited in the plasma, on which current conducting electrons will scatter, providing an increase in thermal power released in the current channel, an increase in thermal emission current, plasma fluxes from the cathode and anode. Conditions will arise for the multiplication of explosive electron emission center. The capture of a few electrons emitted by these centers into the current channel plasma is already capable of creating conditions for the formation of a cathode spot and the development of a spark discharge. Thus, increasing the power put in the auxiliary discharge can accelerate the transition to an independent high-current discharge in the commutated gap by increasing the initial concentration of free electrons due to the ionization of the residual gas. However, an increase in the concentration of free electrons due to plasma dispersion from the surface discharge region can only be expected at distances from the ignition point to the main discharge gap of no more than 0.25 cm.

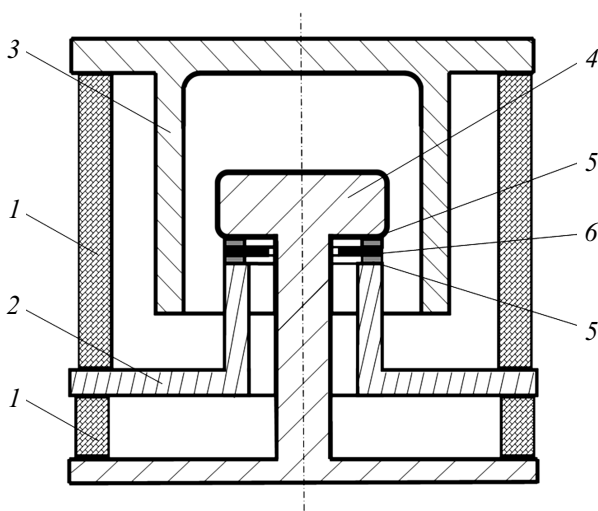


Figure 5. The basic design of a compact vacuum spark discharger: 1 — dielectric sealed shell, 2 — ignition electrode, 3 — anode, 4 — cathode, 5 — secondary metal bushings, 6 — dielectric washer.

2. Experiments with compact vacuum spark discharger

The flux density of ionizing radiation and fast electrons from the auxiliary discharge plasma can be tried to increase by increasing the energy put into the auxiliary discharge. In this way it is possible to influence the discharger delay in the direction of its reduction and to compensate for its dependence on the residual gas pressure.

Relevant studies have been carried out using compact controlled vacuum dischargers, which are a three-electrode coaxial system with the main elements being the anode, cathode, ignition electrode and a dielectric washer separating the cathode and ignition electrode (Fig. 5). The discharge unit is housed in a sealed dielectric enclosure, evacuated to a pressure no worse than 10^{-1} Pa.

The electrodes were made of aluminum alloy and the dielectric washer was made of 0.1 mm thick mica. The diameter of the inner cylindrical electrode (cathode) is 5 mm. The outer electrode (anode) is in the form of a hollow cylinder and has an inner diameter of 7 mm. Additional metal sleeves, each 0.1 mm thick and of corresponding diameter, are placed coaxially between the dielectric washer and the adjacent electrodes, between the dielectric washer and the ignition electrode — covar, between the dielectric washer and the cathode — covar and titanium. The ignition electrode, the nearest cathode edge, additional metal spacers and the dielectric washer together make up the ignition assembly.

The discharger operating at 1.5 kV at the cathode–anode gap was chosen as the test piece. Using the previously described ignition scheme, the delay current switched by the discharger varied chaotically between 200 and 1500 ns. By changing the capacitive energy store rating,

it was possible to increase the current reached in the ignition unit to 110 A. The energy in the capacitive storage of the ignition unit varied from $5 \cdot 10^{-5}$ to $6 \cdot 10^{-2}$ J. The energy stored in the external switched circuit was invariably 0.6 J. As the energy in the ignition circuit increased, the auxiliary discharge was delayed. The results show that increasing the energy input to the auxiliary discharge at the spark stage gives the most tangible reduction in delay time. The energy invested in the auxiliary discharge was determined by calculation based on measurements of current and voltage dynamics in the discharge.

In order to analyze the recorded delay variation, delay distribution diagrams were plotted at different energy levels of the ignition circuit. The diagrams are delay distribution functions normalized to the total number of switching operations (Fig. 6). They allow you to visually assess the magnitude of the delay and its stability, and to visualize the

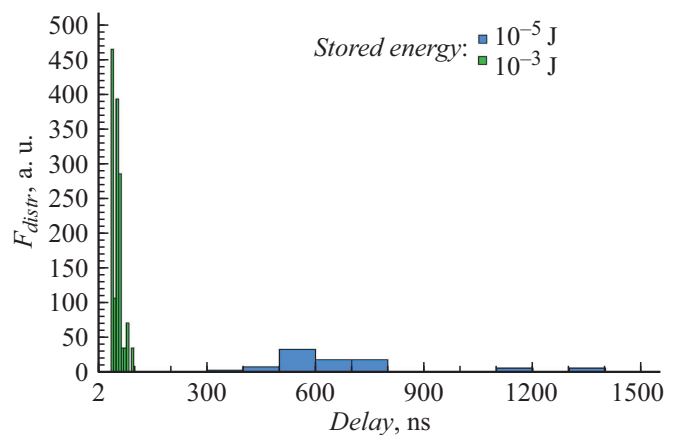


Figure 6. Comparison of the delay distribution diagrams for the ignition scheme with energy in the accumulator $E = 1 \cdot 10^{-5}$ J and the scheme with $E = 1 \cdot 10^{-3}$ J.

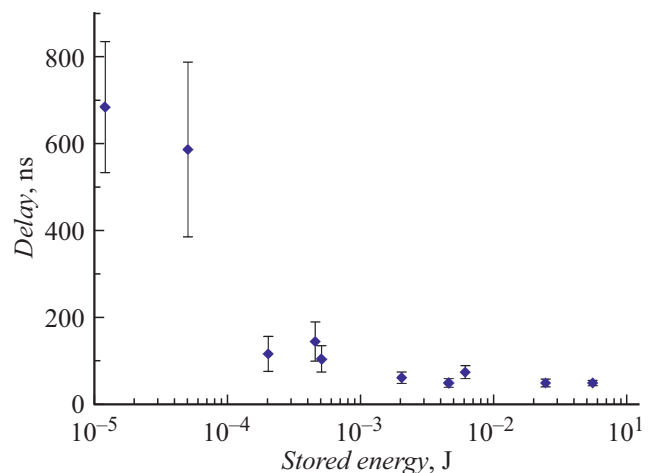


Figure 7. Dependence of the arcing delay in the cathode–anode gap on the energy stored in the ignition circuit

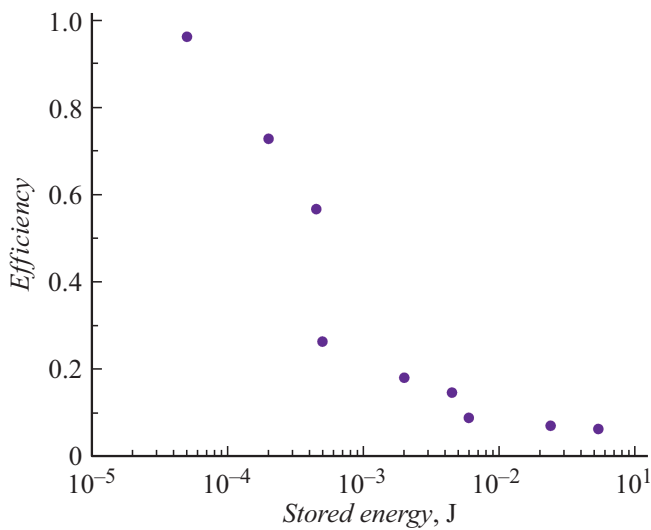


Figure 8. Diagram of the proportion of energy put in the initiating discharge commutation process as a function of the energy stored in the ignition circuitry.

change in the delay distribution function depending on the energy level of the ignition circuit.

These measurements have shown that it is possible, by increasing the ignition energy used, not only to reduce the delay time of the discharger (Fig. 7), but also to make the discharger more stable by reducing the variation in the values recorded.

At the same time, the results of these studies have shown that the degree of influence on the delay time decreases with increasing pulse width of the current flowing over the dielectric surface (Fig. 8). The latter circumstance seems to be due to the fact that as the duration of the auxiliary discharge increases, the relative duration of its arc stage increases, the transition to which is accompanied by a rapid drop in the power released in the discharge channel.

3. Conclusion

Based on the analysis of the experimental data obtained, the short vacuum gap switching process using an auxiliary spark discharge can be represented as follows. The initial stage is the ionization of the residual gas in the commutated gap by shortwave radiation and fast electrons from the plasma of the auxiliary discharge, with the predominance of electron impact ionization. When the initial concentration of free charge carriers is below some threshold, there is likely to be an initial low-current volumetric discharge, which then contracts and becomes a spark discharge, evolving into an arc. If the initial concentration of free electrons is above the threshold concentration, a spark discharge without an intermediate stage becomes possible.

As the energy supplied to the ignition circuit of the small vacuum spark gaps increases, there is a steady decrease in the delay time of the gaps and an increase in the level of

delay stability. This can be attributed to an increase in the initial concentration of free electrons in the main discharge gap and a corresponding decrease in the transition time to an independent high-current discharge.

The most efficient, in terms of minimization and stability of the discharger delay time, is the investment of energy in the formation of the initiating plasma during the spark stage of the auxiliary discharge over the dielectric surface in the ignition assembly.

Conflict of interest

The authors declare that they have no conflict of interest.

References

- [1] A. Anders. *Cathodic Arcs* (Springer Series on Atomic, Optical, and Plasma Physics, NY., 2008), DOI: 10.1007/978-0-387-79108-1
- [2] A. Batrakov, S. Popov, N. Vogel, B. Juttner. *IEEE Transactions on Plasma Science*, **31** (5), 817 (2003). DOI: 10.1109/TPS.2003.818427
- [3] G.A. Mesyats *Explosive electron emission* (Fizmatlit, M., 2011)
- [4] A.P. Babichev, N.A. Babushkina, A.M. Bratkovsky, M.E. Brodov, M.V. Bystrov, B.V. Vinogradov, L.I. Vinokurova, E.P. Gelman, A.P. Geppe, I.S. Grigoryev, K.G. Gurtovoy, V.S. Egorov, A.V. Eletsy, L.K. Zarembo, V.Y. Ivanov, V.L. Ivashintseva, V.V. Ignatiev, R.M. Imamov, A.V. Inyushkin, N.V. Kadobnova, I.I. Karasik, K.A. Kikoin, V.A. Krivoruchko, V.M. Kulakov, S.D. Lazarev, T.M. Lifshits, Yu.E. Lubarsky, S.V. Marin, I.A. Maslov, E.Z. Meilikhov, A.I. Migachev, S.A. Mironov, A.L. Musatov, Yu.P. Nikitin, L.A. Novitsky, A.I. Obukhov, V.I. Ozhogin, R.V. Pisarev, Yu.V. Pisarevsky, V.S. Ptuskin, A.A. Radzig, V.P. Rudakov, B.D. Summ, R.A. Sunyaev, M.N. Khlopin, I.N. Khlustikov, V.M. Cherepanov, A.G. Chertov, V.G. Shapiro, V.M. Shustriakov, S.S. Yakimov, V.P. Yanovsky. *Physical quantities: Handbook*, ed. by Ye.S. Grigoriyev, Ye.Z. Meylikhov. (Energoizdat, Moscow, 1991)
- [5] S.G. Davydov, A.N. Dolgov, A.V. Korneev, R.Kh. Yakubov. *Technical Physics Letters* **45** (12), 33 (2019). DOI: 10.21883/TP.2022.15.55262.153-21
- [6] S.G. Davydov, A.N. Dolgov, A.S. Katorov, V.O. Revazov, R.Kh. Yakubov. *Applied Physics*, **1**, 39 (2021). DOI: 10.51368/1996-0948-2021-1-39-43
- [7] H.C. Miller. *IEEE Transactions on Dielectrics and Electrical Insulation*, **22** (6), 3641 (2015). DOI: 10.1109/14.231534
- [8] Raiser Yu.P. *Physics of Gas Discharge* (Nauka, M., 1992).
- [9] S.A. Barentgolts, D.L. Shmelev, I.V. Uimanov. *IEEE Transactions on Plasma Science*, **43** (8), 2236 (2015). DOI: 10.1109/TPS.2015.2431321
- [10] E.V. Parkevich, M.A. Medvedev, A.I. Khiryanova, G.V. Ivanenkov, A.V. Agafonov. In collection: *Electrophysical and Optical Processes in Plasma and Solid State Media and Nanostructures*, ed. G.A. Mesyats. (RUSAINS, M., 2019), p. 217.